The ISME Journal (2014) 8, 409–417

www.nature.com/ismej

ORIGINAL ARTICLE

# Coordinated transporter activity shapes high-affinity iron acquisition in cyanobacteria

Chana Kranzler[1,2], Hagar Lis[2,3], Omri M Finkel[1], Georg Schmetterer[4], Yeala Shaked[2,3] and Nir Keren[1]

[1]*Department of Plant and Environmental Sciences, The Alexander Silberman Institute of Life Sciences, Hebrew University of Jerusalem, Jerusalem, Israel;* [2]*Interuniversity Institute for Marine Sciences in Eilat, Eilat, Israel;* [3]*The Freddy and Nadine Herrmann Institute of Earth Sciences, Hebrew University of Jerusalem, Jerusalem, Israel and* [4]*Institute of Physical Chemistry, University of Vienna, Vienna, Austria.*

**Iron bioavailability limits biological activity in many aquatic and terrestrial environments. Broad scale genomic meta-analyses indicated that within a single organism, multiple iron transporters may contribute to iron acquisition. Here, we present a functional characterization of a cyanobacterial iron transport pathway that utilizes concerted transporter activities. Cyanobacteria are significant contributors to global primary productivity with high iron demands. Certain cyanobacterial species employ a siderophore-mediated uptake strategy; however, many strains possess neither siderophore biosynthesis nor siderophore transport genes. The unicellular, planktonic, freshwater cyanobacterium, *Synechocystis sp.* PCC 6803, employs an alternative to siderophore-based uptake-reduction of Fe(III) species before transport through the plasma membrane. In this study, we combine short-term radioactive iron uptake and reduction assays with a range of disruption mutants to generate a working model for iron reduction and uptake in *Synechocystis sp.* PCC 6803. We found that the Fe(II) transporter, FeoB, is the major iron transporter in this organism. In addition, we uncovered a link between a respiratory terminal oxidase (Alternate Respiratory Terminal Oxidase) and iron reduction - suggesting a coupling between these two electron transfer reactions. Furthermore, quantitative RNA transcript analysis identified a function for subunits of the Fe(III) transporter, FutABC, in modulating reductive iron uptake. Collectively, our results provide a molecular basis for a tightly coordinated, high-affinity iron transport system.**

*The ISME Journal* (2014) **8,** 409–417; doi:10.1038/ismej.2013.161; published online 3 October 2013
**Subject Category:** Geomicrobiology and microbial contributions to geochemical cycles
**Keywords:** cyanobacteria; iron; transport

## Introduction

Iron limitation is a challenge common to both terrestrial and aquatic ecosystems. It is of particular importance to photosynthetic organisms who must maintain iron-rich photosynthetic machinery (Raven *et al.*, 1999; Blaby-Haas and Merchant, 2012). Indeed, iron availability limits primary productivity in many aquatic habitats, including one-third of the world's oceans (Martin *et al.*, 1991; Boyd *et al.*, 2007).

Iron bioavailability is determined by its concentration and speciation. In oxygenated environments, Fe(II) is rapidly oxidized to Fe(III). Unlike the readily soluble Fe(II), Fe(III) rapidly precipitates as poorly available ferrioxyhydroxides (for $Fe(OH)_3$, $K_{so} = 10^{-37.5}$ $M^4$ (Byrne and Kester, 1976)). The remaining dissolved fraction is dominated by organic complexation, where Fe-binding compounds help maintain iron in solution (Hunter and Boyd, 2007). Total dissolved Fe concentrations in aquatic environments are in the nanomolar to subnanomolar range (Johnson *et al.*, 1997).

Cyanobacteria are Gram-negative photosynthetic prokaryotes that contribute significantly to global primary productivity (Falkowski, 1997). Cyanobacterial iron transport systems must contend with limited Fe bioavailability in order to meet their iron requirements (Shaked and Lis, 2012). As is the case with many other prokaryotes, a siderophore-mediated iron uptake strategy is commonly attributed to cyanobacteria. In this strategy, cells synthesize and secrete siderophores-low molecular weight compounds that are highly specific for Fe(III) (Neilands, 1981). Once bound to iron, the ferrisiderophore complex is transported through the outer and plasma membranes before the iron is released from the complex (Braun and Hantke, 2011).

Correspondence: N Keren, Department of Plant and Environmental Sciences, The Alexander Silberman Institute of Life Sciences, Edmond J Safra Campus, Givat Ram, Hebrew University of Jerusalem, Jerusalem 91904, Israel.
E-mail: Nir.ke@mail.huji.ac.il
Received 12 June 2013; revised 1 August 2013; accepted 17 August 2013; published online 3 October 2013

Siderophore biosynthesis and ferrisiderophore transporters were characterized in a range of cyanobacterial species (Goldman *et al.*, 1983; Wilhelm, 1995; Ito and Butler, 2005; Stevanovic *et al.*, 2012; Kranzler *et al.*, 2013). However, many cyanobacteria, most notably open ocean strains, possess neither siderophore biosynthesis nor siderophore transport capabilities (Hopkinson and Morel, 2009), alluding to an alternative iron acquisition strategy.

Reductive iron uptake is a transport strategy in which iron substrates undergo reduction from Fe(III) to Fe(II) before transport. This pathway is well-characterized in eukaryotic phytoplankton (Jones *et al.*, 1987; Soria-Dengg and Horstmann, 1995; Maldonado and Price, 2001; Shaked *et al.*, 2005; Allen *et al.*, 2007; Morrissey and Bowler, 2012) and involves plasma membrane reductases that promote the reductive dissociation of organically bound Fe(III). In contrast to substrate-specific siderophore-mediated iron uptake, this strategy grants phytoplankton access to a wide range of organic and inorganic Fe(III) complexes.

Among cyanobacteria, the analysis of both laboratory cultures and natural populations suggested the existence of a reductive iron uptake pathway (Rose and Waite, 2005; Lis and Shaked, 2009). In a previous work we demonstrated that the unicellular cyanobacterium, *Synechocystis sp.* PCC 6803 (henceforth *Synechocystis* 6803), employs a reductive iron uptake strategy for a range of substrates including Fe–siderophore complexes and free inorganic iron (Fe′) (Kranzler *et al.*, 2011). Like many ecologically relevant *Synechococcus* and *Prochlorococcus* strains, it does not possess any known siderophore biosynthesis genes (Hopkinson and Morel, 2009).

Although a molecular pathway for siderophore-mediated iron uptake was characterized in the siderophore producer *Anabaena sp.* PCC 7120 (Stevanovic *et al.*, 2012), the mechanism of iron transport in non-siderophore producers is not well-established. Several *Synechocystis* 6803 proteins were shown to have a role in iron transport through the plasma membrane. Katoh *et al.* (2001) identified the gene products of *futA*, *futB* and *futC* as the components of a FutABC transporter, involved in the transport of inorganic Fe(III) (Table 1). This transporter is made up of a soluble Fe(III)-binding periplasmic component (FutA), a permease (FutB) and a membrane associated ATPase (FutC) (Katoh *et al.,* 2001). Two FutA homologs, FutA1 and FutA2, were identified and shown to bind Fe(III) (Katoh *et al.*, 2001; Badarau *et al.*, 2008). In addition, a protein homologous to the *Escherichia coli* Fe(II) transporter, FeoB (Kammler *et al.*, 1993), was shown to be involved in Fe(II) acquisition (Table 1, Katoh *et al.*, 2001).

The role of these transporters in the reductive iron uptake pathway employed by *Synechocystis* 6803 was not investigated. Furthermore, the source of reducing power required for reductive iron uptake is unknown. In this work we explore the molecular nature of iron reduction and transport. We present a detailed study of mutant strains for several of the aforementioned genes. On the basis of short-term iron transport and reduction assays complemented with quantitative RNA transcript analysis, we suggest a working model for the molecular mechanism of reductive iron uptake in *Synechocystis* 6803.

## Materials and methods

*Trace metal clean techniques*

In order to avoid iron contamination of experimental solutions, all plastic and glass ware was washed in HCl. Stock solutions were prepared using analytical grade chemicals and double distilled water (18.2 mΩ). For short-term experiments, all preparation and experimental work was done in a clean room facility. For these experiments, all plastic ware was washed in HCl and in EDTA before use.

*Growth conditions*

*Synechocystis* 6803 was grown in YBG11 with constant shaking at 30 °C under 60 μmol photons $m^{-2} s^{-1}$ (Kranzler *et al.*, 2011). Culture growth was monitored in a Cary 300 spectrophotometer (Varian, Palo Alto, CA, USA) at 730 nm. As the correlation between optical density and cell numbers varied between wild-type and mutant strains, cell densities were determined using hemocytometer cell counts. Iron was added precomplexed with EDTA (in twofold excess) at 0.1 μM for Fe-deplete medium

**Table 1** Mutant strains

| *Mutant strain* | *Disrupted gene* | *Assigned function* | *Assigned location* | *Reference* | *Color code* |
|---|---|---|---|---|---|
| Δ*futA1* | *slr1295* | Fe(III)-binding protein | Cytoplasmic and thylakoid membranes | 30–32 | Blue |
| Δ*futA2* | *slr0513* | Fe(III)-binding protein | Periplasm | 27, 28 | Blue |
| Δ*futA1*Δ*futA2* | *slr0513*, *slr1295* | | | 27 | Blue |
| Δ*futC* | *sll1878* | Fe(III) transport ATP-binding protein | Peripheral plasma membrane | 27 | Blue |
| Δ*ARTO* | *slr2082*, *slr2083* | Cytochrome c oxidase homolog | Integral plasma membrane | 33, 34 | Orange |
| Δ*feoB* | *slr1392* | Fe(II) transporter | Plasma membrane | 27 | Green |

The table summarizes all of the mutant strains used in this study, the disrupted genes, assigned function and location based on previous work. For clarity, each transporter and mutant was assigned a color code that is used throughout this work.

and 10 μM for Fe-replete medium. Iron was kept in solution by applying 16 μM of the trace metal buffer, EDTA, which prevents iron precipitation on cell surfaces and maintains a computable pool of free, inorganic Fe(III) (Fe′) through dissociation and complexation reactions. FeEDTA is not bioavailable to *Synechocystis* 6803 (Kranzler *et al.*, 2011).

Before the transfer into Fe-deplete medium, cells were spun down and washed twice in YBGll medium with no added iron. Mutant strains for genes used in this work are described in Table 1.

*Short-term experiments*

In YBG11 medium, Fe′ is an excellent substrate for reduction by the cell and is transported with remarkable affinity ($K_m = 0.27$ nM) by a pathway that is upregulated by Fe limitation (Kranzler *et al.*, 2011). Therefore, we chose to use an Fe′ experimental system (buffered by the Fe(III) chelator, EDTA) as a model with which to probe the molecular nature of iron reduction and transport processes. Assays were conducted with cultures in the logarithmic phase of growth, 2 days after transfer into Fe-deplete medium. This amount of time was sufficient to upregulate iron responsive genes in the wild-type (Singh *et al.*, 2003; Hernandez-Prieto *et al.*, 2012).

*Uptake and reduction assays*

Short-term radioactive experiments were conducted in YBG11 medium supplemented with precomplexed 75–100 nM $^{55}$FeEDTA. Precomplexation reactions were performed with a twofold excess of EDTA and adjusted to pH 5–7 to ensure complex stability. Carrier FeEDTA was supplemented to a final concentration of ~150 nM Fe, amounting to a total of 0.19 nM Fe′. EDTA was added to a final concentration of 16 μM. Medium was buffered at pH 7.8 (10 mM Hepes) in the absence of trace minerals in order to minimize iron contamination. Where indicated, the Fe(II)-specific chelator, Ferrozine (FZ),was added to a final concentration of 200 μM. Uptake and reduction experiments were run in the dark at 30 °C as described previously (Kranzler *et al.*, 2011). Measurements were taken three to four times over the course of each experiment with a duplicate measurement at the first and final time points. When only three measurements were taken, the middle point was also measured in duplicates. Iron uptake and reduction rates were calculated from the linear regression of the data. Examples of raw data are presented in Figure 1.

*RNA extraction and reverse transcription*

RNA was extracted from wild-type and mutant cultures 8 h after transfer to Fe-deplete medium (TRI Reagent, Molecular Research Center Inc., Cincinnati, OH, USA). Sampling time was selected based on the recent finding that maximal transcription of many Fe-limitation genes is reached after 12 h of Fe-limitation (Hernandez-Prieto *et al.*, 2012). RNA was treated with TURBO DNAse-I, DNA-free (Ambion, Carlsbad, CA, USA). Reverse transcription reactions were performed with 0.5 μg RNA using the RevertAid M-Mul V R everse Transcriptase (Thermo Scientific, Rockford, IL, USA) and random hexamer primers (Thermo Scientific).

*Quantitative PCR assays*

Quantitative real-time PCR was performed using a Rotor-Gene 6000 Thermal Cycler (Corbett Research, Brisbane, Australia). Amplifications were carried out in triplicate using ABsolut Blue SYBR Green ROX (Thermo Scientific, ABgene, Rockford, IL, USA). Primer sequences used in this analysis are described in Supplementary Table S1. Primer amplification efficiency was determined using standard curve dilutions. A no-template reaction was used as a negative control. Melting curve analysis confirmed the specificity of each reaction. Quantitative real-time PCR was performed with RNA to verify that detectable DNA was removed from each sample. Transcript abundances were examined relative to the expression of the control gene *rnpb*.

## Results

*Analysis of Fe reduction and uptake rates in mutant strains*

Our previous work demonstrated that *Synechocystis* 6803 employs a reductive iron uptake strategy (Kranzler *et al.*, 2011). In this pathway, cell-mediated reduction of Fe(III) to Fe(II) occurs before transport through the plasma membrane. The Fe(II)-specific chelator, FZ, was applied in order to probe for the formation of an Fe(II) intermediate. When reductive iron uptake is at play, FZ binds biologically produced Fe(II). This results in the inhibition of Fe transport and enables the quantification of Fe(III) reduction rates (measured by $Fe(II)FZ_3$ formation rates; Shaked *et al.*, 2005). Reductive iron acquisition is deduced from a strong inhibitory effect of FZ on uptake rates, coupled to an Fe(III) reduction rate that corresponds to the degree of inhibition. We have used this approach to analyze wild-type and several mutant strains (Table 1) in order to identify the molecular components of the reductive iron uptake pathway.

We measured Fe′ uptake and reduction rates and tested the effect of FZ on uptake in each strain (Figures 1 and 2). Three distinct phenotypes were observed in the mutants analyzed in this study (Figure 1). (i) Δ*FutC* showed impaired Fe transport as compared with the wild-type (Figures 1a, b). Δ*FutA2,* Δ*FutA1FutA2* and Δ*ARTO* also displayed a similar phenotype (Supplementary Figure S1). (ii) Δ*FutA1* showed higher uptake than the

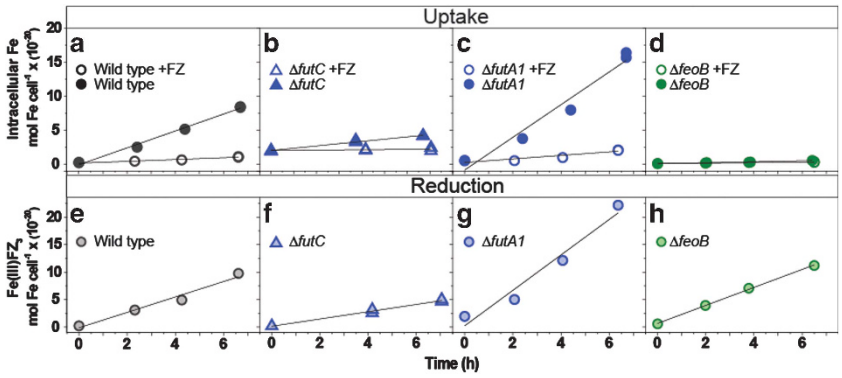


**Figure 1** Short-term radioactive iron uptake and reduction experiments. Representative uptake (**a–d**) and reduction (**e–h**) assays were conducted with strains: wild-type (**a**, **e**), Δ*futC* (**b**, **f**), Δ*futA1* (**c**, **g**) and Δ*feoB* (**d**, **h**). Medium contained free, inorganic Fe(III), supplied in the form of $^{55}$FeEDTA. Iron uptake and reduction rates reported in the manuscript were calculated from the linear regression of these data.

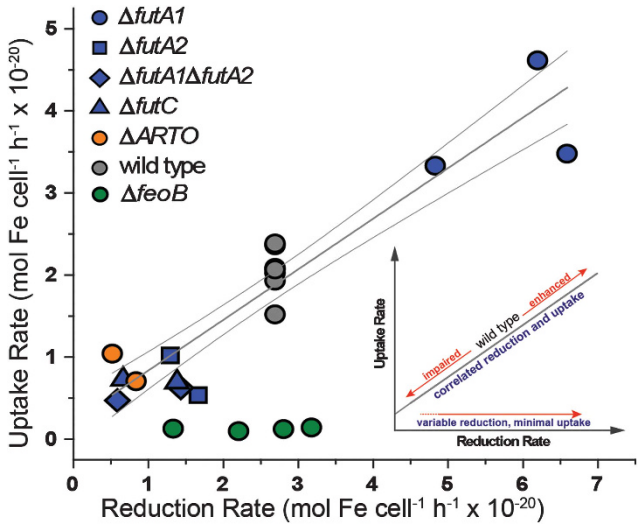


**Figure 2** Analysis of uptake and reduction rates. Fe uptake rates were plotted as a function of reduction rates. Because uptake and reduction rates sometimes vary, each set of experiments contained a wild-type culture for reference. The wild-type uptake rates were 1.1—3.8 × $10^{-20}$ mol Fe $cell^{-1}h^{-1}$and the wild-type reduction rates were 1.3–4.9 × $10^{-20}$ mol Fe $cell^{-1}h^{-1}$. For each experiment, mutant rates were normalized to internal wild-type reduction rates. Values are presented relative to the average wild-type reduction rate (2.7 × $10^{-20}$ mol Fe $cell^{-1}h^{-1}$). Each point represents an independent biological repeat. Each mutant was tested at least twice. Two separate mutant strains for *feoB* were tested ($n=4$). Δ*futA1* results, that clusters away from the other strains, was tested an additional time ($n=3$). In all strains except Δ*feoB*, uptake rates plot linearly as a function of reduction rates ($y=0.62x+2.2\times10^{-21}$, $r^2=0.88$). Gray lines are 90% confidence bands enclosing the linear regression. Correlations between reduction and uptake rates in the data set are highlighted schematically (insert).

wild-type (Figure 1c). These phenotypes were reproducible in independent biological repeats (Supplementary Figure S1). As with the wild-type, strains exhibiting these two phenotypes were similarly inhibited by FZ (80–90%, Supplementary Figure S1 insert). Fe(III) reduction rates were measured in parallel (Figures 1e–g). Each of these strains exhibited an Fe reduction rate that was high enough to account for the inhibition of uptake by FZ (Figure 1). On the basis of these results, we suggest that these mutants employ a reductive iron uptake strategy under our experimental conditions. (iii) The third phenotype was found in Δ*feoB,* which exhibited exceptionally slow uptake rates that were unaffected by FZ (Figure 1d). Interestingly, Δ*feoB* displayed an Fe reduction rate comparable to that of the wild-type (Figure 1h).

We found that mutants with faster or slower Fe reduction rates than the wild-type also had proportionally faster or slower uptake rates. The ratio between uptake and reduction rates remained constant in the wild-type and five of the six strains examined, as evident from the linear correlation in Figure 2. As Fe reduction occurs before transport through the plasma membrane (Kranzler *et al.*, 2011), this finding suggests that the phenotypes observed in these mutants stem from changes in Fe reduction rather than Fe uptake capacity. It is important to note that all experiments were conducted at subsaturating iron concentrations (Kranzler *et al.*, 2011), that is, the iron uptake *capacities* were higher than the measured iron uptake *rates*. Therefore, changes in reduction capacity will be reflected by higher or lower uptake rates. When following the trendline in Figure 2, data points above the wild-type have enhanced reduction capabilities, whereas those below the wild-type are impaired in these capabilities (Figure 2, insert). Only one mutant, Δ*feoB,* falls below the trendline as its reduction rates were comparable to the wild-type but its uptake rates remained minimal.

The very slow iron uptake rates measured in Δ*feoB* remained unaffected by FZ (Figure 1d, Supplementary Figure S1), suggesting that there is no transport of Fe(II) in this mutant despite its moderate to normal reduction capabilities (Figures 1h and 2). On the basis of these data, we suggest that FeoB functions as the major iron transporter under our experimental conditions and that its substrate is Fe(II).

*Iron reduction: a role for respiration*

We considered the cellular processes likely to be involved in iron reduction. As Fe′ uptake and reduction rates were unaffected by light (Kranzler *et al.*, 2011), it is unlikely that photosynthetic electron flow is relevant. In addition, experiments with wild-type cells incubated with the photosynthetic inhibitor, 3-(3,4-dichlorophenyl)-1,1-dimethylurea (DCMU), did not affect Fe uptake rates but caused an increase in iron reduction rates (Supplementary Figure S2). As both photosynthetic and respiratory chains in cyanobacteria share a quinone/quinol pool (Schmetterer *et al.*, 1994), the inhibition of photosynthesis may increase respiratory electron flow through Cyt$b_6f$. Does respiratory electron flow have a role in reductive iron uptake?

The *Synechocystis* 6803 genome contains three respiratory terminal oxidases. Two of these—a cytochrome c oxidase (Cox) and a quinol oxidase (Cyd)—are important in cellular respiration (Alge and Peschek, 1993; Schmetterer *et al.*, 1994; Howitt and Vermaas, 1998). The function of the third, the Alternate Respiratory Terminal Oxidase (ARTO), or CtaII, remained unclear. Mutant strains defective in both *cox* and *cyd* genes exhibited very little respiratory activity, suggesting that ARTO does not reduce oxygen under the conditions tested (Howitt and Vermaas, 1998; Pils and Schmetterer, 2001). In order to determine whether ARTO is involved in the reductive iron uptake pathway, we measured iron uptake and reduction rates in the Δ*ARTO* mutant strain.

Δ*ARTO* displayed markedly impaired Fe reduction and uptake rates as compared with wild-type (Figure 2) indicating that ARTO is indeed involved in reductive iron uptake. As Δ*ARTO* plots linearly with the wild-type and the other mutants (Figure 2), it is likely that its phenotype stems from diminished iron reduction capabilities.

*FutABC and reductive iron uptake*

The predominance of reductive iron uptake in *Synechocystis* 6803 raised questions regarding the function of the Fe(III) transporter, FutABC. Δ*FutA2,* Δ*FutC* and Δ*FutA1*Δ*FutA2* displayed impaired iron reduction and uptake capabilities (Figure 2). The Δ*FutA1* mutant exhibited significantly enhanced Fe reduction and uptake rates as compared with the wild-type (Figures 1 and 2). Interestingly, as with Δ*ARTO,* these phenotypes also fall on the linear regression characteristic of the strains that use reductive iron uptake (Figure 2). What role might FutABC subunits have in this pathway?

We hypothesized that these subunits modulate Fe reduction capability. FutA2 is the most prominent Fe(III)-binding protein in the periplasm (Badarau *et al.*, 2008). It is possible that formation of the Fe(III)FutA2 complex maintains the concentration gradient that drives external Fe′ into the periplasm. This gradient could not be established in Δ*futA2*, decreasing the available substrate for reduction and uptake (Figure 2). FutC and FutA1 were both identified as intracellular proteins (Katoh *et al.*, 2001; Tolle *et al.*, 2002; Srivastava *et al.*, 2005) rendering their location better suited for regulatory interactions (Tetsch and Jung, 2009; Ohashi *et al.*, 2011; Richet *et al.*, 2012).

Transcriptional changes in *futA2* and *feoB* were measured in Δ*FutA1* and Δ*FutC* mutants 8 h after transfer into Fe-deplete medium (Figure 3). Transcription of many iron transport-related genes is strongly induced by iron depletion within this time period. The transcript levels of *futA2, futA1, futC* and *feoB* are upregulated at least 2.5-fold following transition to iron limitation (Hernandez-Prieto *et al.*, 2012). Quantitative PCR analysis showed that *feoB* transcript levels were higher in both strains as compared with wild-type (Figure 3). The effect was more pronounced in Δ*FutC* despite its impaired uptake and reduction rates (Figure 3 and Supplementary Figure S3). Interestingly, *futA2* transcript abundance did correspond to Fe reduction and uptake rates in the different strains (Figure 3 and Supplementary Figure S3). Transcript levels were higher in Δ*FutA1* and lower in Δ*FutC* as compared with wild-type (Figure 3 and Supplementary Figure S3). These data suggest that the observed phenotypes in Δ*FutC* and Δ*FutA1* (Figures 1 and 2) stem from modifications of the regulatory network in the absence of these subunits.

## Discussion

In this study, we examined the molecular pathway by which Fe is reduced and transported in the unicellular, non-siderophore-producing cyanobacterium, *Synechocystis* 6803. On the basis of our analysis of mutant strains (Figures 1–3) and the location of each protein (Table 1) we propose a working model for reductive iron uptake in *Synechocystis* 6803 (Figure 4).

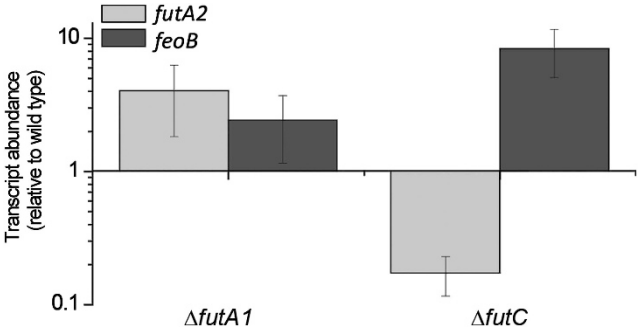


**Figure 3** Quantitative real-time PCR (qRT-PCR) analysis. *futA2* and *feoB* transcription were quantified in wild-type, Δ*futA1* and Δ*futC* 8 h after transfer into Fe-deplete medium. Transcript levels were internally normalized to the control gene, *rnpB*. The data are presented as compared with the wild-type. Error bars represent two biological repeats. Fe uptake and reduction rates in Δ*futA1* and Δ*futC* are plotted as a function of *futA2* and *feoB* transcript abundance.

Our data suggest that the ARTO in *Synechocystis* 6803 has a role in reductive iron uptake (Figures 1 and 2). It is interesting to note that it was suggested that ARTO functions under microaerobic conditions; directly upstream of the ARTO operon is a binding site for an oxygen responsive transcriptional regulator, responsible for activating anaerobic metabolism (Howitt and Vermaas, 1998). Dissimilatory metal reducing bacteria utilize extracellular Fe(III) as the terminal electron acceptor in anaerobic respiration (Schroder *et al.*, 2003). In dissimilatory iron reduction electrons are transferred outside of the cell, in certain cases through pili structures (Shi *et al.*, 2007; Richter *et al.*, 2012). Although this mode of iron reduction might be the evolutionary progenitor of assimilatory reductive iron uptake, we were unable to identify homologs of the multiheme cytochromes that are involved in dissimilatory iron reduction in the *Synechocystis* 6803 genome.

It is likely that uptake-associated iron reduction occurs inside the periplasmic space in close proximity to electron sources and iron transporters. The *Synechocystis* 6803 ARTO is located exclusively in the plasma membrane (Pils and Schmetterer, 2001; Berry *et al.*, 2002), a location that could facilitate the supply of electrons for the reduction of periplasmic Fe(III) (Figure 4). ARTO genes were also found in most cyanobacteria with multiple copies in certain diazotropic organisms (Hart *et al.*, 2005).

In reductive iron uptake, Fe(III) is transported through the outer membrane of the cell (Figure 4). Some cyanobacteria have tonB-dependent transporters that shuttle iron through the outer membrane (Stevanovic *et al.*, 2012; Kranzler *et al.*, 2013), but there is no evidence of such a function for the tonB-dependent transporters identified in *Synechocystis* 6803 (Katoh *et al.*, 2001). It is also possible that Fe′ diffuses through nonspecific porins in the outer membrane (Fujii *et al.*, 2011). Upon entering the periplasm FutA2 binds Fe(III), generating the chemical gradient that facilitates the influx of Fe. This is consistent with the suggested role for FutA2 in metal partitioning in the periplasm (Waldron *et al.*, 2007). On the basis of our findings (Figures 2 and 3), FutA2 is a major factor in determining iron reduction and subsequent transport. Given its abundance, the Fe(III)FutA2 complex may be a substrate for reduction. Structural analysis of the protein revealed that it is made up of two domains that clamp Fe(III) via five coordinating ligands (Badarau *et al.*, 2008). FutA2 is a high-affinity Fe(III)-binding protein with only residual Fe(II) binding capabilities (Badarau *et al.*, 2008). The reduction of Fe(III)FutA2 would therefore result in the release of Fe(II).

Following reduction, Fe(II) is transported through FeoB, the major iron transporter under our experimental conditions (Figure 4). In Δ*feoB*, iron uptake rates are minimal but are nevertheless well within the detection limit (Figures 1 and 2). Katoh *et al.* (2001) found that Δ*feoB* growth was similar to the wild-type when transferred from Fe-rich medium to medium without added iron. However, it is important to note that the transfer from Fe-rich medium to Fe-free conditions probes the internal iron storage that accumulated before the transfer rather than Fe transport capability under iron limitation (Keren *et al.*, 2004; Shcolnick *et al.*, 2007).

Furthermore, iron uptake rates in Δ*feoB* were unaffected by FZ (Figure 1 and Supplementary Figure S1). This indicates the presence of an additional Fe uptake pathway that does not involve reduction, for which FutABC is a likely candidate.

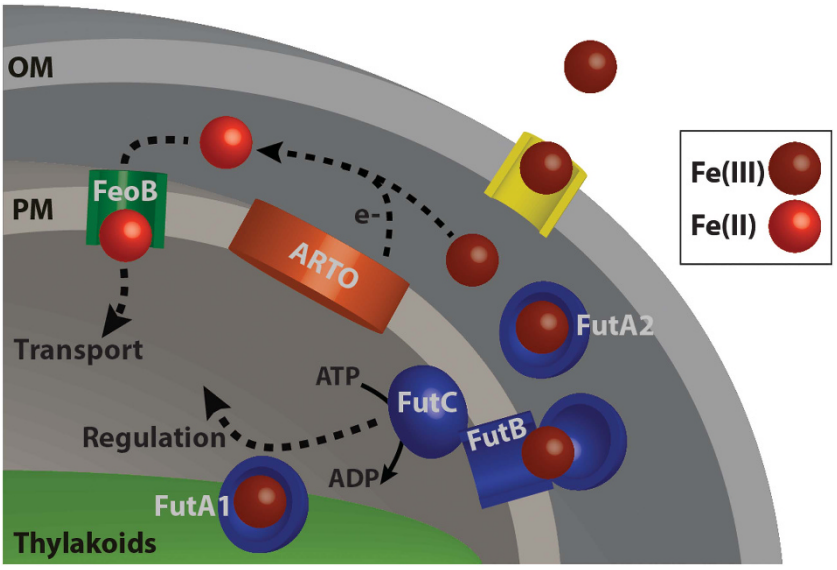


**Figure 4** A working model for the reductive iron uptake pathway. In reductive iron uptake, Fe(III) is first transported through the outer membrane (OM) of the cell (yellow). FutA2 (blue) binds periplasmic Fe(III). The respiratory terminal oxidase, ARTO (orange), is involved in Fe(III) reduction before transport through the plasma membrane (PM). The resulting Fe(II) is transported through FeoB (green). Intracellular subunits FutA1 and FutC of the Fe(III) transporter, FutABC (blue), regulate the reductive iron uptake pathway.

These results are consistent with the iron uptake experiments conducted by Katoh *et al.* (2001) that implicated FutABC in Fe(III) transport but also demonstrated that Fe(II) transport was significantly faster than Fe(III) transport. That work also reported severely impaired uptake of Fe(II) in Δ*feoB*.

The disruption of FutABC genes yielded mutant phenotypes that retained the ratio between iron reduction and uptake rates observed in the wild-type (Figure 2). Fe reduction and transport rates combined with transcriptional profiles in Δ*FutC* and Δ*FutA1* suggest a regulatory function for these intracellular subunits (Figure 4). There is evidence to suggests that ABC transporters are used as co-sensors for signal transduction in bacteria (Tetsch and Jung, 2009). For example, the maltose transporter MalEFGK sequesters the MalT transcriptional regulator (Richet *et al.*, 2012). In cyanobacteria, the ATP-binding subunit of the NRT-ABC nitrate/nitrite transporter is required for the regulation of ammonium promoted inhibition of transport (Ohashi *et al.*, 2011). Furthermore, a similar function for a FutABC subunit may have been retained in vascular plant chloroplasts. FutC is the only remaining subunit of the cyanobacterial iron transport system in plants. Inactivation of a FutC ortholog (atNAP14) in *Arabidopsis thaliana* resulted in impaired iron homeostasis (Shimoni-Shor *et al.*, 2010). Although it is likely that FutABC is a functional Fe(III) transporter, our findings demonstrate a role for FutABC subunits in the modulation of reductive iron uptake.

Siderophore synthesis and transport genes are absent from many cyanobacterial genomes (Hopkinson and Morel, 2009) raising the possibility of additional iron transport pathways. Reductive iron uptake constitutes an alternative to siderophore-mediated uptake that is advantageous in dilute heterogeneous environments (Volker and Wolf-Gladrow, 1999).

Our experimental conditions singled out the reductive iron uptake pathway and enabled the identification of its components in *Synechocystis* 6803. The composition of Fe transporters analyzed here is not unique. Many microorganisms possess the genetic potential for multiple iron transporters (Rivers *et al.*, 2009; Desai *et al.*, 2012; Hopkinson and Barbeau, 2012; Morrissey and Bowler, 2012). Bioinformatic analyses of iron transport genes revealed that fut genes are common in cyanobacteria (Rivers *et al.*, 2009; Hopkinson and Barbeau, 2012, with additional analysis included in Supplementary Figure S4). Feo genes were identified in freshwater and coastal cyanobacteria but were notably absent from marine picocyanobacteria (Palenik *et al.*, 2006; Rivers *et al.*, 2009; Desai *et al.*, 2012; Hopkinson and Barbeau, 2012; Supplementary Figure S4). However, many of the marine picocyanobacteria strains did possess a broad-specificity divalent metal transporter, the natural resistance-associated macrophage protein (Hopkinson and Barbeau, 2012), suggesting the potential for Fe(II) transport. An additional divalent metal transporter, ZIP (ZRT-, IRT-like protein), was also identified (Hopkinson and Barbeau, 2012). Both natural resistance-associated macrophage protein and ZIP have important roles in the acquisition of a wide range of divalent metals including Zn(II), Co(II), Fe(II), Mn(II) and Cd(II) (Nevo and Nelson, 2006; Taudte and Grass, 2010). These transporters were also identified in some freshwater and coastal cyanobacteria (Supplementary Figure S4).

The widespread genetic potential for Fe(II) transport suggests that reductive iron uptake may be employed by other cyanobacteria. The occurrence of several distinct transporters in a single organism necessitates coordination in order to acquire iron efficiently. The reductive iron uptake mechanism elucidated here in *Synechocystis* 6803 provides a model for coordinated transporter function.

## Conflict of Interest

The authors declare no conflict of interest.

## Acknowledgements

We thank Terou Ogawa for generously sharing mutant strains with us. This work was supported by the Israeli Science Foundation (grant no. 806/11). GS acknowledges financial support from 'Projekt Chlorophyll'.

## References

Alge D, Peschek GA. (1993). Identification and characterization of the ctac (coxb) gene as part of an operon encoding subunit-I, subunit-II, and subunit-III of the cytochrome c oxidase (cytochrome aa3) in the cyanobacterium Synechocystis PCC 6803. *Biochem Biophys Res Co* **191**: 9–17.

Allen MD, del Campo JA, Kropat J, Merchant SS. (2007). FEA1, FEA2, and FRE1, encoding two homologous secreted proteins and a candidate ferrireductase, are expressed coordinately with FOX1 and FTR1 in iron-deficient *Chlamydomonas reinhardtii*. *Eukaryot Cell* **6**: 1841–1852.

Badarau A, Firbank SJ, Waldron KJ, Yanagisawa S, Robinson NJ, Banfield MJ *et al.* (2008). FutA2 is a ferric binding protein from *Synechocystis* PCC 6803. *J Biol Chem* **283**: 12520–12527.

Berry S, Schneider D, Vermaas WFJ, Rögner M. (2002). Electron transport routes in whole cells of *Synechocystis* sp strain PCC 6803: The role of the cytochrome bd-type oxidase. *Biochemistry* **41**: 3422–3429.

Blaby-Haas CE, Merchant SS. (2012). The ins and outs of algal metal transport. *BBA-Mol Cell Res* **1823**: 1531–1552.

Boyd PW, Jickells T, Law CS, Blain S, Boyle EA, Buesseler KO *et al.* (2007). Mesoscale iron enrichment experiments. 1993-2005: Synthesis and future directions. *Science* **315**: 612–617.

Braun V, Hantke K. (2011). Recent insights into iron import by bacteria. *Curr Opin Chem Biol* **15**: 328–334.

Byrne RH, Kester DR. (1976). Solubility of hydrous ferric oxide and iron speciation in seawater. *Mar Chem* **4**: 255–274.

Desai DK, Desai FD, LaRoche J. (2012). Factors influencing the diversity of iron uptake systems in aquatic microorganisms. *Front Microbiol* **3**: 362.

Falkowski PG. (1997). Photosynthesis: The paradox carbon dioxide efflux. *Curr Bio* **7**: R637–R639.

Fujii M, Dang TC, Rose AL, Omura T, Waite TD. (2011). Effect of light on iron uptake by the freshwater cyanobacterium *Microcystis aeruginosa*. *Environ Sci & Technol* **45**: 1391–1398.

Goldman SJ, Lammers PJ, Berman MS, Sandersloehr J. (1983). Siderophore-mediated iron uptake in different strains of Anabaena sp. *J Bacteriol* **156**: 1144–1150.

Hart SE, Schlarb-Eidley BG, Bendall DS, Howe CJ. (2005). Terminal oxidases of cyanobacteria. *Biochem Soc Trans* **33**: 832–835.

Hernandez-Prieto MA, Schon V, Georg J, Barreira L, Varela J, Hess WR *et al.* (2012). Iron deprivation in *Synechocystis*: inference of pathways, non-coding RNAs, and regulatory elements from comprehensive expression profiling. *G3(Bethesda)* **2**: 1475–1495.

Hopkinson BM, Barbeau KA. (2012). Iron transporters in marine prokaryotic genomes and metagenomes. *Environ Microbiol* **14**: 114–128.

Hopkinson BM, Morel FMM. (2009). The role of siderophores in iron acquisition by photosynthetic marine microorganisms. *Biometals* **22**: 659–669.

Howitt CA, Vermaas WFJ. (1998). Quinol and cytochrome oxidases in the cyanobacterium *Synechocystis* sp. PCC 6803. *Biochemistry* **37**: 17944–17951.

Hunter KA, Boyd PW. (2007). Iron-binding ligands and their role in the ocean biogeochemistry of iron. *Environ Chem* **4**: 221–232.

Ito Y, Butler A. (2005). Structure of synechobactins, new siderophores of the marine cyanobacterium *Synechococcus sp* PCC 7002. *Limnol and Oceanogr* **50**: 1918–1923.

Johnson KS, Gordon RM, Coale KH. (1997). What controls dissolved iron concentrations in the world ocean? *Mar Chem* **57**: 137–161.

Jones GJ, Palenik BP, Morel FMM. (1987). Trace metal reduction by phytoplankton - the role of plasmalemma redox enzymes. *J Phycol* **23**: 237–244.

Kammler M, Schön C, Hantke K. (1993). Characterization of the ferrous iron uptake system of *Escherichia coli*. *J Bacteriol* **175**: 6212–6219.

Keren N, Keren N, Aurora R, Pakrasi HB. (2004). Critical roles of bacterioferritins in iron storage and proliferation of cyanobacteria. *Plant Physiol* **135**: 1666–1673.

Katoh H, Hagino N, Ogawa T. (2001). Iron-binding activity of FutA1 subunit of an ABC-type iron transporter in the cyanobacterium Synechocystis sp. strain PCC 6803. *Plant Cell Physiol* **42**: 823–827.

Katoh H, Hagino N, Grossman AR, Ogawa T. (2001). Genes essential to iron transport in the cyanobacterium *Synechocystis s*p. strain PCC 6803. *J Bacteriol* **183**: 2779–2784.

Kranzler C, Lis H, Shaked Y, Keren N. (2011). The role of reduction in iron uptake processes in a unicellular, planktonic cyanobacterium. *Environ Microbiol* **13**: 2990–2999.

Kranzler C, Rudolf M, Keren N, Schleiff E. (2013). in Advances in Botanical Research: Genomics of Cyanobacteria. Chauvat Franck, Chauvat Corinne Cassier (eds). Vol. 65. Elsevier Ltd: Amsterdam, the Netherlands, pp 57–105.

Lis H, Shaked Y. (2009). Probing the bioavailability of organically bound iron: a case study in the Synechococcus-rich waters of the Gulf of Aqaba. *Aquat Microb Ecol* **56**: 241–253.

Maldonado MT, Price NM. (2001). Reduction and transport of organically bound iron by *Thalassiosira oceanica* (Bacillariophyceae). *J Phycol* **37**: 298–309.

Martin JH, Gordon RM, Fitzwater SE. (1991). The Case for Iron. *Limnol and Oceanogr* **36**: 1793–1802.

Morrissey J, Bowler C. (2012). Iron utilization in marine cyanobacteria and eukaryotic algae. *Front Microbiol* **3**: 1–13.

Neilands JB. (1981). Iron absorption and transport in microorganisms. *Annu Rev Nutr* **1**: 27–46.

Nevo Y, Nelson N. (2006). The NRAMP family of metal-ion transporters. *BBA-Mol Cell Res* **1763**: 609–620.

Ohashi Y, Shi W, Takatani N, Aichi M, Maeda S, Watanabe S *et al.* (2011). Regulation of nitrate assimilation in cyanobacteria. *J Ex Bot* **62**: 1411–1424.

Palenik B, Ren Q, Dupont CL, Myers GS, Heidelberg JF, Badger JH *et al.* (2006). Genome sequence of *Synechococcus* CC9311: Insights into adaptation to a coastal environment. *PNAS* **103**: 13555–13559.

Pils D, Schmetterer G. (2001). Characterization of three bioenergetically active respiratory terminal oxidases in the cyanobacterium *Synechocystis* sp strain PCC 6803. *FEMS Microbiol Lett* **203**: 217–222.

Raven JA, Evans MCW, Korb RE. (1999). The role of trace metals in photosynthetic electron transport in O2 evolving organisms. *Photosynthesis Res* **60**: 111–149.

Richet E, Davidson AL, Joly N. (2012). The ABC transporter MalFGK2 sequesters the MalT transcription factor at the membrane in the absence of cognate substrate. *Mol Microbiol* **85**: 632–647.

Richter K, Schicklberger M, Gescher J. (2012). Dissimilatory reduction of extracellular electron acceptors in anaerobic respiration. *Appl Environ Microb* **78**: 913–921.

Rivers AR, Jakuba RW, Webb EA. (2009). Iron stress genes in marine Synechococcus and the development of a flow cytometric iron stress assay. *Environ Microbiol* **11**: 382–396.

Rose AL, Waite TD. (2005). Reduction of organically complexed ferric iron by superoxide in a simulated natural water. *Environ Sci & Technol* **39**: 2645–2650.

Schmetterer G, Alge D, Gregor W. (1994). Deletion of cytochrome-C-oxidase genes from the cyanobacterium *Synechocystis* sp PCC 6803 - evidence for alternative respiratory pathways. *Photosynth Res* **42**: 43–50.

Schroder I, Johnson E, de Vries S. (2003). Microbial ferric iron reductases. *FEMS Microbiol Rev* **27**: 427–447.

Shaked Y, Lis H. (2012). Disassembling iron availability to phytoplanktonl. *Front Microbio* **3**: 1–26.

Shaked Y, Kustka AB, Morel FMM. (2005). General kinetic model for iron acquisition by eukaryotic phytoplankton. *Abstr Pap Am Chem* **S229**: U891–U891.

Shcolnick S, Shaked Y, Keren N. (2007). A role for mrgA, a DPS family protein, in the internal transport of Fe in the cyanobacterium *Synechocystis* sp. PCC 6803. *Biochim Biophys Acta* **1767**: 814–819.

Shi L, Squier TC, Zachara JM, Fredrickson JK. (2007). Respiration of metal (hydr)oxides by Shewanella and Geobacter: a key role for multihaem c-type cytochromes. *Mol Microbiol* **65**: 12–20.

Shimoni-Shor E, Hassidim M, Yuval-Naeh N, Keren N. (2010). Disruption of Nap14, a plastid-localized non-intrinsic ABC protein in *Arabidopsis thaliana* results in the over-accumulation of transition metals and in aberrant chloroplast structures. *Plant Cell Environ* **33**: 1029–1038.

Singh AK, McIntyre LM, Sherman LA. (2003). Microarray analysis of the genome-wide response to iron deficiency and iron reconstitution in the cyanobacterium *Synechocystis* sp PCC 6803. *Plant Physiol* **132**: 1825–1839.

Soria-Dengg S, Horstmann U. (1995). Ferrioxamines B and E as iron sources for the marine diatom *Phaeodactylum tricornutum*. *Mar Ecol-Prog Ser* **127**: 269–277.

Srivastava R, Pisareva T, Norling B. (2005). Proteomic studies of the thylakoid membrane of *Synechocystis* sp PCC 6803. *Proteomics* **5**: 4905–4916.

Stevanovic M, Hahn A, Nicolaisen K, Mirus O, Schleiff E. (2012). The components of the putative iron transport system in the cyanobacterium *Anabaena* sp PCC 7120. *Environ Microbiol* **14**: 1655–1670.

Taudte N, Grass G. (2010). Point mutations change specificity and kinetics of metal uptake by ZupT from *Escherichia coli*. *Biometals* **23**: 643–656.

Tetsch L, Jung K. (2009). The regulatory interplay between membrane-integrated sensors and transport proteins in bacteria. *Mol Microbiol* **73**: 982–991.

Tolle J, Michel KP, Kruip J, Kahmann U, Preisfeld A, Pistorius EK *et al.* (2002). Localization and function of the IdiA homologue slr1295 in the cyanobacterium *Synechocystis* sp strain PCC 6803. *Microbiol Sgm* **148**: 3293–3305.

Volker C, Wolf-Gladrow DA. (1999). Physical limits on iron uptake mediated by siderophores or surface reductases. *Mar Chem* **65**: 227–244.

Waldron KJ, Tottey S, Yanagisawa S, Dennison C, Robinson NJ. (2007). A periplasmic iron-binding protein contributes toward inward copper supply. *J Biol Chem* **282**: 3837–3846.

Wilhelm SW. (1995). Ecology of iron-limited cyanobacteria: A review of physiological responses and implications for aquatic systems. *Aquat Microb Ecol* **9**: 295–303.

Supplementary Information accompanies this paper on The ISME Journal website (http://www.nature.com/ismej)